Quantum Photonics Vibrometer for Vibration-based Damage Detection

Álvaro Romero Mato[1, 2], Yunhyeok Han[1, 2], Malvika Garikapati[3], Vahid Yaghoubi[1, 2]
[1]Q-VAIbe group, Aerospace Structures and Materials, Faculty of Aerospace Engineering, Delft University of Technology, Delft, Netherland
[2]Aerospace Structures and Materials, Faculty of Aerospace Engineering, Delft University of Technology, Delft, Netherlands
[3]Quantum Computing Inc, Hoboken (New Jersey), USA

Abstract Recent advances in quantum photonics and single-photon detection are enabling new sensing capabilities for vibration-based diagnostics and non-destructive evaluation. This work investigates the signal characteristics and effective resolution of the Quantum Photonic Vibrometer (QPV), a quantum-enhanced, non-contact sensor designed for sub-nanometric vibration measurements in Structural Health Monitoring (SHM).
The QPV operates at a telecom wavelength of 1550 nm using a mode-locked laser emitting 20 MHz optical pulses, combined with time-gated photon detection on an avalanche photodiode (APD). The measured photon-count signal arises from phase-induced speckle modulation, where structural vibrations modulate the optical phase of the backscattered field, producing measurable intensity fluctuations.
In this study, photon-count time series obtained from aluminum specimens (pure and with artificial defects) are analyzed using time- and frequency-domain techniques, including Fast Fourier Transform (FFT), sliding Root Mean Square (RMS), variance, and Hilbert envelope extraction. A simplified physical model is introduced to relate photon-count fluctuations to vibration-induced phase variations, providing insight into the effective measurement resolution in the presence of photon shot noise.
Results show that pure aluminum exhibits stable and low-variance responses with consistent spectral signatures, while defective samples introduce measurable changes in frequency content and signal variability. These observations indicate that the QPV signal contains physically meaningful information related to structural condition, and that its sensitivity is governed by the interplay between speckle-induced phase modulation and photon-count statistics.
This work highlights the potential of QPV as a sensing modality for vibration analysis and defect-sensitive diagnostics, establishing a foundation for data-driven structural health monitoring using quantum-enhanced vibrometry.

Keywords: Quantum photonic vibrometer; Structural health monitoring; Single-photon detection; Speckle modulation; Vibration analysis; Signal processing

https://doi.org/10.58286/33944

Introduction

Structural Health Monitoring (SHM) relies on accurate and sensitive measurement techniques to detect changes in the mechanical response of materials and structures. Among these, vibration-based diagnostics play a central role, as structural defects often manifest as changes in dynamic behavior, including shifts in resonance frequencies and damping [1, 2].

Classical vibration measurement systems, such as Laser Doppler Vibrometers (LDVs), provide high-resolution, non-contact measurements by detecting Doppler frequency shifts in reflected laser light [3]. While these systems are well-established, they typically rely on continuous-wave operation and require sufficient optical power and stable reflective conditions, which may limit their applicability in low-signal or optically challenging environments [3, 4].

Recent advances in quantum photonics and single-photon detection have opened new possibilities for vibration sensing beyond classical paradigms [5]. In particular, time-gated single-photon detection enables the measurement of optical signals at extremely low light levels, offering enhanced sensitivity in challenging conditions [6]. The Quantum Photonic Vibrometer (QPV) leverages these capabilities by encoding structural vibrations into photon-count fluctuations arising from coherent light scattering. Unlike classical vibrometry techniques that directly measure velocity through frequency shifts, the QPV detects variations in the intensity of backscattered light caused by speckle modulation, which is highly sensitive to small phase changes induced by structural motion [7]. As a result, the measured photon-count signal provides an indirect but information-rich representation of the underlying vibration.

Despite its potential, the interpretation of photon-count-based vibrometry signals remains largely unexplored. In particular, the relationship between photon-count fluctuations, vibration amplitude, and measurement resolution is not yet fully understood.

In this work, we investigate the physical and statistical properties of QPV signals and analyze their sensitivity to structural changes using both time- and frequency-domain techniques.

1. Measurement Principle and Resolution

1.1 Measurement Principle

The operation of the QPV follows the chain from mechanical displacement to photon-count fluctuations. The incident laser field is described as a coherent electromagnetic wave. In optical measurements, it is sufficient to describe the electric field, as it directly determines the detected intensity. A monochromatic field can be written as

$$E(x,t) = E_0 \cos(kx - \omega t + \phi_0),$$

where $k = 2\pi/\lambda$. The phase is the argument of the cosine and determines the position of the wave within its oscillation cycle. A change in optical path length produces a phase shift. In reflection geometry, a surface displacement $x(t)$ leads to

$$\Delta\phi(t) = \frac{4\pi}{\lambda} x(t), \tag{1}$$

which is a standard result in interferometric measurements [7, 8].

In a classical LDV, the detected signal is obtained by interfering a reference beam with the reflected beam. The intensity is directly given by

$$I(t) \propto A_r^2 + A_s^2 + 2A_rA_s\cos\big(\phi(t)\big),$$

which shows a single controlled cosine dependence on the phase difference. The measured signal is therefore a continuous interferometric waveform.
In contrast, the QPV operates on light scattered from a rough surface. The detected field is the superposition of many contributions

$$E(t) = \sum_k A_k e^{i\phi_k(t)},$$

leading to an intensity

$$I(t) \propto \sum_k |A_k|^2 + \sum_{k\neq j} A_kA_j\cos\big(\phi_k(t) - \phi_j(t)\big).$$

The signal is therefore not a single cosine but the sum of many interference terms with different phase differences. These phases depend on the scattering paths and produce a speckle pattern. When the surface vibrates, all phases vary according to the phase–displacement relation, resulting in intensity fluctuations rather than a single oscillation.
In the QPV, these intensity variations are detected using a time-gated avalanche photodiode (APD), producing a photon-count time series

$$x(t) \to \Delta\phi(t) \to I(t) \to N(t)$$

1.2 Resolution Analysis

Although both LDV and QPV follow the same phase–displacement relation (Eq. 1), their resolution is determined by different measurement processes.

In LDV, the phase is measured directly through interference, and the minimum detectable displacement is set by the smallest resolvable phase variation

$$x_{\text{min}}^{\text{LDV}} = \frac{\lambda}{4\pi}\,\Delta\phi_{\text{min}}.$$

The limitation arises from phase noise, including electronic noise and laser stability [3, 4].

In the QPV, the phase is not measured directly. Instead, the signal is obtained from photon counts, which follow Poisson statistics with intrinsic fluctuations

$$\sigma_N = \sqrt{N}.$$

A displacement produces a variation in counts

$$\Delta N \approx S\,x,$$

where $S = dN/dx$ is the system sensitivity (counts per unit displacement). Detectability requires $\Delta N > \sqrt{N}$, leading to

$$x_{\text{min}}^{\text{QPV}} \sim \frac{\sqrt{N}}{S}.$$

To provide a quantitative reference, consider $\lambda = 1550$ nm, for which $\lambda/(4\pi) \approx 123$ nm/rad.

The resolution in both systems can therefore be expressed as

$$x_{\text{min}}^{\text{LDV}} = \frac{\lambda}{4\pi} \Delta\phi_{\text{min}} \quad | \quad x_{\text{min}}^{\text{QPV}} \sim \frac{\sqrt{N}}{S}.$$

A phase variation of $\Delta\phi_{\text{min}} = 10^{-2}$ rad corresponds to a very small shift of the interference waveform, approximately 1.6×10^{-3} of a full 2π cycle. At $\lambda = 1550$ nm, this translates into a displacement on the order of 1 nm, meaning that the LDV detects extremely small temporal shifts in the interference signal.

In the QPV, the measurement is governed by photon-count statistics. The quantity N denotes the mean number of detected photons per measurement window, so repeated measurements yield values such as $N = 10^4 \pm 100$. The sensitivity S describes how many counts change per nanometer of displacement.

For example, if $N = 10^4$, the shot noise is $\sqrt{N} = 100$. If $S = 10^2$ counts/nm, a displacement of 1 nm produces $\Delta N \approx 100$, which is at the noise level. Increasing the sensitivity to $S = 10^3$ counts/nm produces $\Delta N \approx 1000$ counts for the same displacement, clearly above the noise and corresponding to a resolution on the order of 0.1 nm. Increasing N further reduces the relative fluctuations and improves detectability.

Both techniques therefore share the same physical origin, but differ in how the phase is accessed. In LDV, the limit is set by phase resolution in a coherent interference signal, whereas in the QPV it is set by photon-counting statistics and experimentally determined sensitivity. While the wavelength λ defines a common physical scale, the practical resolution of the QPV depends strongly on measurement conditions such as photon flux and system calibration. This reflects two distinct regimes: a phase-limited regime in interferometry and a photon-statistics-limited regime in single-photon detection [4, 5, 6].

2. Experimental Setup

The experimental configuration is designed to excite the sample mechanically while measuring its vibration response. The sample is positioned directly in front of the vibrometer at a distance of approximately 1 m, aligned with the optical axis of the collimator to ensure consistent illumination and backscattered signal collection. The measurement is performed in a reflection geometry, where the laser beam is directed onto the surface and the scattered light is detected by the system.

Mechanical excitation was applied using an external speaker placed near the sample without physical contact. Each sample was excited using an external audio signal generated by a speaker placed near the specimen without physical contact.

The QPV operates at a $\lambda = 1550$ nm using a mode-locked laser source emitting optical pulses at a repetition rate of 20 MHz. The returned signal is detected using an APD operating in Geiger mode, with a gated detection window of approximately 2.4 ns. The system records photon counts for each measurement window, producing a time series that reflects the vibration-induced modulation of the speckle pattern.

3. Results

In this section, we analyze the response of aluminum samples under different mechanical conditions (see Figure 1): pure, Dremel-machined, drilled, and impact-damaged. The objective is to identify characteristic differences in temporal and spectral behavior across these conditions. Each sample was excited using an external acoustic source, and multiple measurements

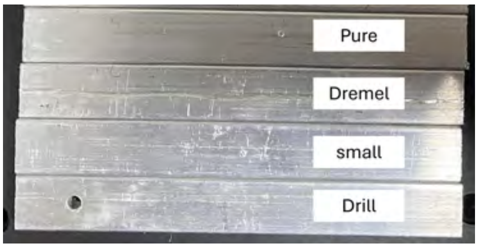

Fig. 1. *Aluminum samples used in the experiments. Artificial defects were introduced by mechanical scratching. Four representative samples are shown, including a reference (pure) specimen and samples with progressively larger defects. These defects are expected to alter the vibrational response of the material.*

(approximately 500 acquisitions) were performed for each condition to ensure statistical consistency.

3.1 Signal Preprocessing

The raw time-domain signals were acquired as photon-count sequences. To enable consistent spectral analysis, the signals were first centered by removing the DC component. A windowing function was then applied prior to computing the Fourier Transform to reduce spectral leakage. The frequency-domain representation was obtained using the Fast Fourier Transform (FFT), and the resulting spectra were normalized to allow comparison across measurements. Additionally, statistical descriptors were computed over time, including the signal envelope obtained via the Hilbert transform, and the root-mean-square (RMS). The envelope captures amplitude modulation, while the RMS provides a measure of the local signal energy, defined as the square root of the time-averaged squared signal.

3.2 Individual Sample Analysis

Figure 2 presents a comparison of the individual sample responses:

3.2.1 Pure Aluminum

The pure sample exhibits a highly stable temporal response. The photon-count signal shows a clear periodic structure, consistent with the dominant low-frequency excitation. This is expected, as the main spectral component is located around 10 Hz, which is sufficiently low to be directly visible in the time-domain signal.

In the frequency domain, the FFT reveals sharp and well-defined peaks at approximately 10, 17, 21, and 29 Hz. These peaks are clearly distinguishable from the background, indicating high signal coherence and efficient coupling between the excitation and the structural response. The envelope and RMS signals remain nearly constant over time, confirming that the energy distribution is stable and that no significant dissipation mechanisms are present. This behavior serves as a baseline reference.

3.2.2 Dremel Machined Surface

The Dremel-machined sample introduces surface irregularities that modify the measured response. In the time domain, the signal appears less regular and more noise-like compared to the pure case. This is not due to noise, but rather to the higher dominant frequency content (around 29–30 Hz), which makes the oscillations less visually distinguishable at the given time scale.

In the frequency domain, the dominant peaks at approximately 10 Hz and 29 Hz are preserved, remaining aligned with the reference peaks identified in the pure sample. However, the intermediate peaks around 17 Hz and 21 Hz are significantly reduced or disappear. This indicates a selective suppression of specific vibration modes due to surface modification. A reduction in the amplitude of the dominant peak around 10 Hz is also observed, suggesting a redistribution of vibrational energy rather than uniform attenuation.

3.2.3 Drilled Sample

The drilled sample exhibits behavior similar to the Dremel case. The presence of a localized defect modifies the vibration response while preserving the dominant excitation structure.

The FFT retains the main peaks at approximately 10 Hz and 29 Hz, consistent with the reference structure of the pure sample, while the intermediate peak around 16–17 Hz is reduced or absent. This confirms that these modes are particularly sensitive to structural perturbations. As in the Dremel case, the time-domain signal appears less regular due to the increased contribution of higher-frequency components. The RMS remains relatively stable, indicating that the global energy distribution is only moderately affected.

3.2.4 Impact-Damaged Sample (Small Hammer)

The impact-damaged sample was created using a small impact hammer (approximately 1/16 inch tip), while the measurement itself was performed under the same acoustic excitation as the other samples. The time-domain signal again exhibits a visible periodic structure, similar to the pure case, consistent with the dominance of lower-frequency components around 10–12 Hz.

In the frequency domain, new spectral features appear. In addition to the main peaks, a strong component emerges near 12 Hz, and additional peaks appear in the 20–25 Hz range. At the same time, the intermediate peaks observed in the pure sample (around 17 Hz and 21 Hz) are no longer clearly present. This deviation from the reference modal structure indicates that the impact damage modifies the system by activating new vibration modes and redistributing spectral energy.

3.3 Comparative Analysis

Figure 3 summarizes the mean spectral and temporal descriptors across all samples, using the pure case as a reference. The dashed vertical lines indicate the dominant peak frequencies identified in the pure sample.

All samples retain the main peaks around 10 Hz and 29–30 Hz, confirming that the primary excitation components are preserved under all conditions. The main differences appear in the intermediate frequency range: the peaks near 16–17 Hz and 21 Hz observed in the pure sample are reduced or disappear in the Dremel and drilled cases, indicating sensitivity of these modes to structural perturbations. A redistribution of spectral energy is also evident, with a decrease in the 10 Hz component and a relative increase near 29–30 Hz in the modified samples. The impact-damaged sample exhibits the largest deviation, with additional components appearing near 12 Hz and in the 20–25 Hz range.

In the time domain, the mean envelope remains similar across all cases, while the RMS provides clearer differentiation. The drilled sample exhibits the highest mean RMS, followed by the Dremel, pure, and impact-damaged samples. The latter also shows increased temporal variability, suggesting a less stable energy distribution.

Overall, structural modifications primarily affect the distribution and activation of vibration modes rather than the fundamental excitation structure.

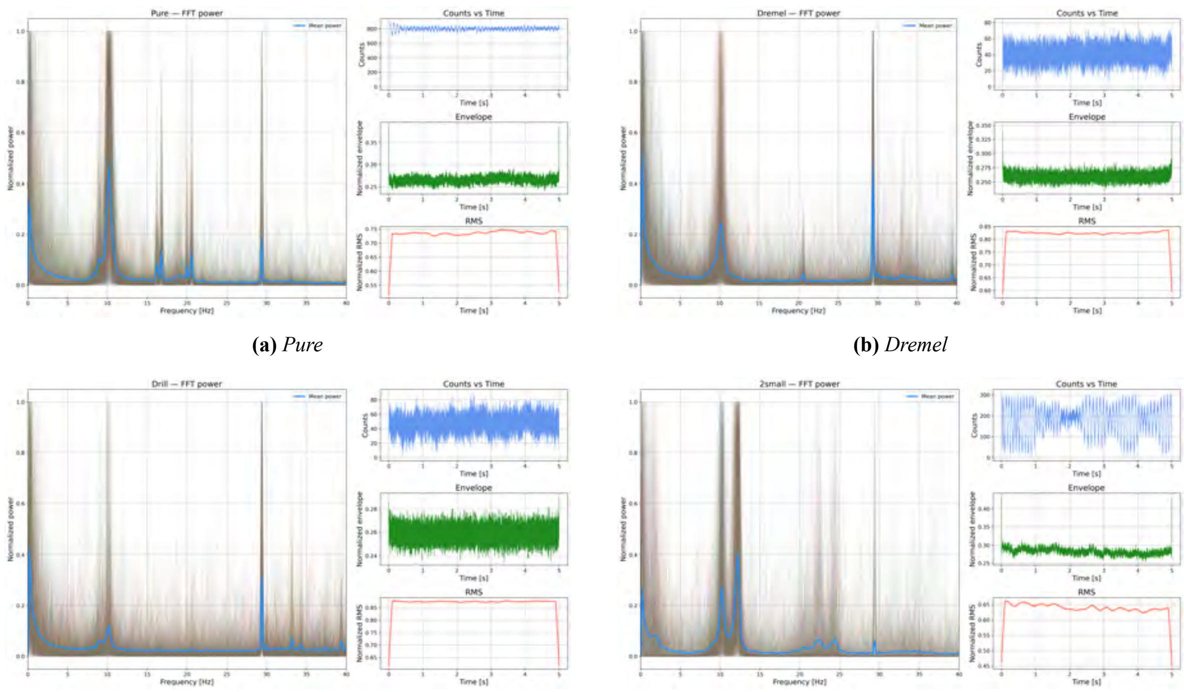

(a) *Pure* **(b)** *Dremel*

(c) *Drill* **(d)** *Impact (small hammer)*

Fig. 2. *Comparison of individual sample responses. Each one shows the time-domain signal, FFT power spectrum, and temporal descriptors (mean envelope and RMS). Differences in spectral content and temporal structure reflect the influence of surface modification and structural damage on the vibrational response.*

4. Conclusion

This work demonstrates the capability of the QPV to capture vibrational signatures in aluminum samples under different structural conditions. Distinct spectral features associated with both excitation and structural response are clearly resolved.
While dominant frequency components remain consistent across samples, structural modifications introduce measurable changes in intermediate modes and energy distribution. This confirms the sensitivity of the method to surface alterations and localized defects.

Overall, the results validate the measurement approach and highlight its potential for vibration-based structural characterization and non-destructive evaluation within structural health monitoring (SHM) applications.

5. Future Work

Future work will focus on optimizing the experimental setup and validating the technique against established methods. In particular, improvements in signal stability, noise reduction, and acquisition parameters are required to enhance resolution and sensitivity. A direct comparison with LDV under identical conditions will be essential to quantitatively assess accuracy and performance.
In addition, further work will aim to better understand the underlying signal formation and sensitivity limits of the method, as well as its robustness under realistic operating conditions. Extending the approach to more complex structures and integrating it into automated SHM pipelines for defect detection and monitoring represent key directions toward practical deployment.

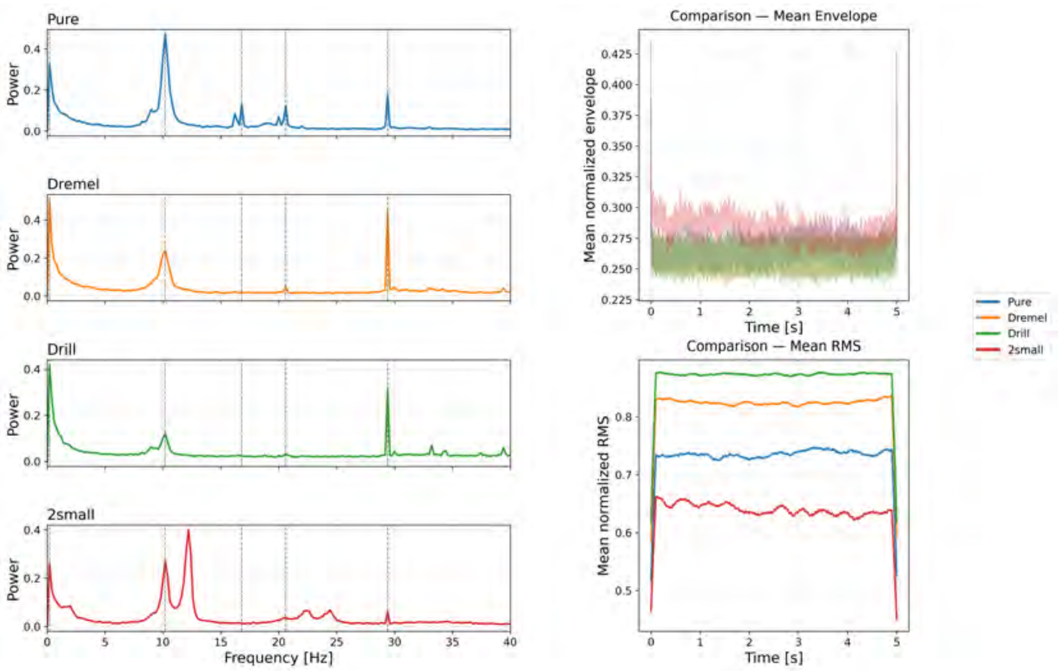

Fig. 3. *Comparison of mean spectral and temporal descriptors across all samples. Left: stacked FFT power spectra, where dashed vertical lines correspond to dominant peak frequencies identified in the pure sample and used as reference. Right: mean envelope and RMS signals. While the envelope remains relatively constant, the RMS highlights differences in energy distribution across samples.*

References

[1] Scott W Doebling, Charles R Farrar, and Michael B Prime. Damage identification and health monitoring of structural and mechanical systems from changes in their vibration characteristics, 1998.

[2] Charles R Farrar and Keith Worden. An introduction to structural health monitoring. *Philosophical Transactions of the Royal Society A*, 365(1851):303–315, 2007.

[3] Paolo Castellini, Gian Marco Revel, and Emilio Tomasini. Laser doppler vibrometry: Development of advanced solutions answering to technology's needs. *Mechanical Systems and Signal Processing*, 20(6):1265–1285, 2006.

[4] S.J. Rothberg, M.S. Allen, P. Castellini, D. Di Maio, J.J.J. Dirckx, D.J. Ewins, B.J. Halkon, P. Muyshondt, N. Paone, T. Ryan, H. Steger, E.P. Tomasini, S. Vanlanduit, and J.F. Vignola. An international review of laser doppler vibrometry: Making light work of vibration measurement. *Optics and Lasers in Engineering*, 99:11–22, 2017. Laser Doppler vibrometry.

[5] Robert H Hadfield. Single-photon detectors for optical quantum information applications. *Nature Photonics*, 3:696–705, 2009.

[6] Matthew D Eisaman, Jingyun Fan, Alan Migdall, and Sergey V Polyakov. Invited review article: Single-photon sources and detectors. *Review of Scientific Instruments*, 82(7), 2011.

[7] Joseph W Goodman. *Speckle Phenomena in Optics: Theory and Applications*. Roberts and Company, 2007.

[8] Bahaa E. A. Saleh and Malvin Carl Teich. *Fundamentals of Photonics*. Wiley, 2019.